Electromagnetic characterization of nonevaporable getter properties between 220–330 and 500–750 GHz for the Compact Linear Collider damping rings

E. Koukovini-Platia,[1,2,*] G. Rumolo,[1] and C. Zannini[1]

[1]*CERN, CH-1211 Geneva, Switzerland*
[2]*EPFL, CH-1015 Lausanne, Switzerland*

Due to its effective pumping ability, nonevaporable getter (NEG) coating is considered for the vacuum chambers of the Compact Linear Collider (CLIC) electron damping rings (EDR). The aim is to suppress fast beam ion instabilities. The electromagnetic (EM) characterization of the NEG properties up to ultrahigh frequencies is required for the correct impedance modeling of the damping ring (DR) components. The properties are determined using rectangular waveguides which are coated with NEG. The method is based on a combination of complex transmission coefficient S_{21} measurements with a vector network analyzer (VNA) and 3D simulations using CST Microwave Studio® (CST MWS). The frequency ranges discussed in this paper are 220–330 and 500–750 GHz.

I. INTRODUCTION

Getters are solid materials capable of chemically pumping gases such as H_2, CO_2, CO, and N_2 after activation. Among different getters, the titanium (Ti), zirconium (Zr), and vanadium (V) alloy has the lowest activation temperature at $180\,°C$ [1,2]. Use of such a coating can help ultrahigh vacuum to be achieved inside an accelerator and can be applied even to very narrow chambers which are hard to pump out with other methods. Specifically, the Compact Linear Collider (CLIC) damping rings (DRs) require an ultrahigh vacuum of 0.1 nTorr pressure.

The nonevaporable getter (NEG) coating can be produced via DC magnetron sputtering [3,4] and the alloy is composed of three intertwisted elemental wires of Ti, Zr, and V. A clean surface for the coating is essential to achieve good adhesion.

CERN had a pioneering role in NEG thin film coating technology [5,6] and has used the technology extensively for the LHC vacuum pipes. Today, however, NEG is widely employed in accelerators and various machines such as ESRF, ELETTRA, and SOLEIL have acquired extensive experience on NEG pumps and coatings. Other synchrotrons such as MAX IV and Sirius are basing the storage ring vacuum pumping mainly on NEG films with more than 95% of the chambers being coated. The use of thin getter films is also foreseen for various future projects such as SLS II, Diamond II, APS upgrade, CLIC damping rings

etc. The typical thickness of NEG films in accelerators is around 1–2 μm.

Although NEG coating technology is widely used nowadays, the impedance of the NEG films has not yet been characterized, with the high frequency regime in particular remaining to be explored. Depending on the bunch length and thus how far in frequency the beam spectrum extends, characterization of the material up to several hundred GHz might be required to be able to assess the resistive wall impedance.

This paper describes the method used to infer the NEG coating properties at frequencies of hundreds of GHz for the first time and also discusses the obtained results.

II. METHOD

For an accurate modeling of the machine impedance, the contribution of vacuum chamber coating to the resistive wall impedance must be taken into account. The short rms bunch length of 1.8 mm in the CLIC DRs extends to hundreds of GHz in the frequency spectrum, therefore it is necessary to characterize the NEG properties up to such high frequencies. The objective is to measure the conductivity of the coated material as a function of frequency.

The proposed method constitutes measuring the radiofrequency (rf) scattering parameters (S-parameters) of a rectangular waveguide employing a vector network analyzer (VNA) as instrumentation and simulating the same waveguide geometry using 3D CST Microwave Studio [7]. The waveguide is a 2-port network that can be described by means of S-parameters as a function of frequency [8]. The loss in the waveguide can be observed from the S_{21} or S_{12} parameter of the scattering matrix. The transmission coefficient S_{21} is related to the waveguide's attenuation, which depends on the material conductivity. The attenuation α of

---
[*]eirini.koukovini-platia@diamond.ac.uk

EM waves in a waveguide can be caused by two factors. First, by the attenuation due to the lossy dielectric material inside the waveguide α_d, and secondly, due to the ohmic losses in the nonperfectly conducting walls α_c [9],

$$\alpha = \alpha_d + \alpha_c. \tag{1}$$

The inner part of the waveguide is filled with air, which is a low-loss dielectric material, thus α_d is negligible and the loss in the waveguide is assumed to be caused only by the conduction loss.

The dependence of S_{21} on the conductivity σ can be obtained by means of Computer Simulation Technology (CST) simulation for a given geometry of waveguide at a specific frequency. The relative permittivity ε_r and permeability μ_r are assumed to be equal to one, while conductivity σ is the unknown parameter scanned in simulations. By intersecting the measured $S_{21}(\mathrm{f})$ parameter with the simulated curve $S_{21}(\sigma)$ at every frequency, the electrical conductivity that matches the measured losses can be extracted at the specific frequency of the measurement. By repeating the intersection over the frequency range of interest, the conductivity can be determined as a function of frequency.

The method has already been successfully benchmarked for frequencies between 10 GHz and 11 GHz (i.e. within the frequency range of the X-band region of the EM spectrum) using a rectangular stainless steel waveguide [10]. The DC conductivity of stainless steel could be determined with an accuracy better than 3% using the described method. The same waveguide was then coated with NEG at CERN and the method was used to characterize NEG conductivity in X-band [10]. The extracted conductivity of 1×10^6 S/m agreed with the measured DC conductivity to about 15%, which is within the uncertainty of the measurement.

III. CHALLENGES OF HIGH FREQUENCY MEASUREMENTS

After demonstrating the validity of the method in X-band, the task of characterizing NEG conductivity at hundreds of GHz was pursued. Several challenges had to be overcome in order to ensure the success of the measurements.

With increasing frequency, the typical procedure of VNA calibration becomes more difficult as does the design of a well-matched load or an open standard. Therefore, calibration methods such as thru-reflect-line (TRL), also used for the X-band measurements [11], become more important at higher frequencies. Moreover, surface roughness starts to have an impact with respect to the transmission losses since the skin depth δ reduces as the frequency increases.

In the frequency range of interest for a conductive material such as NEG with $\sigma > 10^4$ S/m, the skin depth can be calculated with very high accuracy by [12]

$$\delta = \frac{1}{\sqrt{\pi f \mu \sigma}}, \tag{2}$$

where $\mu = \mu_r \mu_0$ is the permeability, μ_r the relative magnetic permeability, μ_0 the permeability of free space, f the frequency, and σ the material conductivity. Last, the mechanical dimensions of the waveguide and the deviation from the ideal ones become critical, thus high manufacturing precision is required.

IV. MEASUREMENTS AT 220–330 GHz

Four 25 mm long aluminum (Al) rectangular waveguides of type WR3.4 were purchased from Virginia Diodes (VDI) for measurements with a bandwidth of 220–330 GHz. In this frequency range only the lowest transverse electric mode TE_{10} is allowed to propagate. The waveguides are produced in two split blocks with an E-plane split and also have a thin gold plating (see Figure 1). The groove dimensions are 0.864 mm in width and 0.432 mm in height with ± 5 μm tolerance.

A. Measurements without NEG coating

As a first test, the transmission coefficient S_{21} was measured without NEG coating and compared to CST simulation of the same geometry waveguide. The comparison is shown in Fig. 2.

The S_{21} transmission along a WR3.4 waveguide agrees very well with the CST simulation as shown in Fig. 2. Some discrepancy is observed mainly after 270 GHz which is further increased with frequency. This is attributed to the surface roughness effect that causes higher losses once it is comparable to the skin depth. For such a good conductor as gold even small amount of roughness can play a role since the skin depth is in the order of 0.168 μm at 220 GHz and 0.137 μm at 330 GHz. The discrepancy remains smaller than 0.7%.

A bare gold waveguide was simulated in CST as the plating is thick enough for the electromagnetic signal to

FIG. 1. WR3.4 (left top and bottom) and WR1.5 (right top and bottom) 25 mm long waveguides from VDI made of Al with thin gold plating.
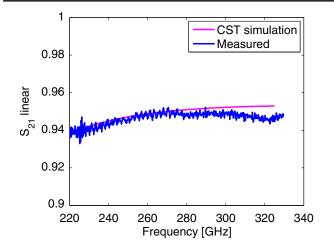
FIG. 2. S_{21} comparison between CST simulation (magenta) for a bare gold waveguide with perfectly smooth surface and S_{21} measurements along the WR3.4 waveguide (blue). In CST simulation the conductivity value used for gold is 4.1×10^7 S/m.

only interact with the gold film. The conductivity used for gold is $\sigma = 4.1 \times 10^7$ S/m, and any surface effects have been neglected in the CST simulations by assuming the surface is smooth. The good agreement between measured and simulated results shown in Fig. 2 demonstrates the possibility to have accurate measurements at such high frequencies. However, it is also evident that the roughness will play a role in this frequency regime. Quantifying the effect of surface roughness is not a trivial task.

The reflection parameter S_{11} was also measured for the WR3.4 waveguide and it is shown in Fig. 3.

The reflection parameter is smaller than -30 dB and therefore its impact on the transmitted signal is expected to be insignificant.

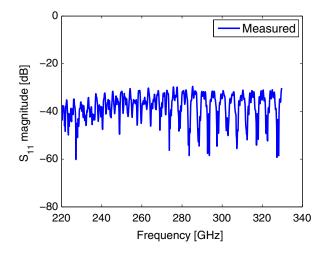The intersection between the measured S_{21} data for the bare gold waveguide and the value found from CST

FIG. 3. S_{11} reflection parameter measured in the WR3.4 waveguide. S_{11} is smaller than -30 dB and the impact on the transmitted signal S_{21} is expected to be negligible.
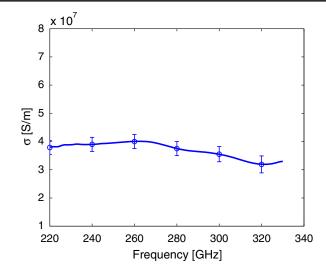

FIG. 4. Effective conductivity of gold between 220–330 GHz as extracted from the intersection of measured S_{21} and CST simulation which assumes a roughness-free waveguide.

simulations can be used to infer the effective conductivity of gold. The conductivity found using this method is shown in Figure 4. For frequencies between 220–270 GHz the agreement with the theoretical conductivity value of 4.1×10^7 S/m is good and only a 5% discrepancy is noted. However, after around 270 GHz a reduction of approximately 22% in conductivity is observed, again reflecting the increased losses due to surface roughness effects.

B. Measurements with NEG coating

The waveguides were rinsed with n-hexane and antidust blowing was applied prior to coating. The NEG coating was applied via magnetron sputtering at CERN, targeting a thickness of 3 μm. The waveguides had to be disassembled into two halves to apply the coating since a wire cannot fit in such a small groove. They were later reassembled at VDI to ensure that they meet the required alignment tolerances. Although the E-plane split of the waveguides is insensitive to gaps of few μm, the two halves were masked to avoid coating outside the groove and especially on the waveguide interface as this could disturb the measurements due to the additional gap with the connector adaptors.

Full two-port S-parameter measurements were realized using a VNA with frequency extenders manufactured by VDI. The measurement set-up is shown in Fig. 5.

In Fig. 6, the transmission parameters S_{21} are plotted for all four WR3.4 waveguides as a function of frequency. They are labeled as 1, 5–12, 5–15, and 5–16. In the same figure, the simulated curve from CST is also shown, assuming DC conductivity of NEG equal to $\sigma = 0.57 \times 10^6$ S/m and a uniform coating profile of 3 μm thickness. The relative permittivity ε_r and permeability μ_r are assumed to be equal to one in the simulation. The NEG
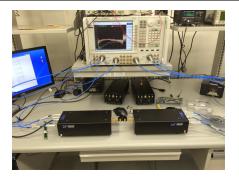
FIG. 5. A WR1.5 rectangular waveguide connected to the VNA with the corresponding frequency extenders.

FIG. 7. Measurements of the reflected parameters S_{11} in all four WR3.4 waveguides. S_{11} is just below -20 dB for waveguides 5–12, 5–15, and 5–16. The matching is significantly better for waveguide 1 with a reflection below -30 dB.

conductivity value used in CST simulations is the average of measurements on NEG-coated glass samples done at CERN. The DC conductivity measurements gave values between 0.5×10^6 S/m and 0.7×10^6 S/m, with a 15% uncertainty [13]. An interesting observation was the difference from the measured DC value using the coating setup deployed for the X-band measurements. In this case the values were between 0.66×10^6 S/m and 1×10^6 S/m. It was concluded that the setup used to apply the coating plays an important role on the elemental composition of the alloy and hence on the resulting DC NEG conductivity.

Figure 6 shows that the measured losses are higher by around 10%, i.e., the measured S_{21} is lower by 10% than the CST result. In CST the assumption was made that the waveguide is smooth, i.e., it has no roughness and that the coating is uniform. Waveguide sample 1 was measured with a different VNA compared to 5–12, 5–15, and 5–16 and the measurements are evidently less noisy compared to the other three. A 10%–15% sample-to-sample variance

characterizes the S_{21} measurements that come from the VNA itself. Transmission was measured in forward and reverse directions by flipping the waveguides by 180°.

The reflection parameters S_{11} were also measured in forward and reverse direction for all four WR3.4 waveguides and the obtained results are shown in Fig. 7. The measured value for S_{11} is just below -20 dB for waveguides 5–12, 5–15, and 5–16. For waveguide sample 1 the reflection is lower, i.e., less than -30 dB, which is a significantly better matching. The worse matching in waveguides 5–12, 5–15, and 5–16 is reflected in the fluctuations observed in Fig. 6 for these waveguides.

The effective conductivity versus frequency is obtained from the intersection between the measured data and values
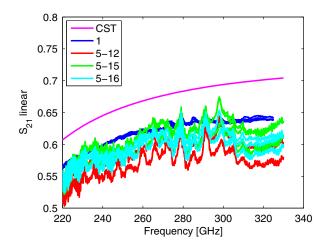

FIG. 6. S_{21} comparison between CST simulation (magenta) for a DC conductivity value of 0.57×10^6 S/m and measurements of four WR3.4 waveguides. Two curves are shown for each waveguide. One curve corresponds to the transmission measured in the forward direction, the other to the transmission measured in the reverse direction by flipping the waveguides by 180°.
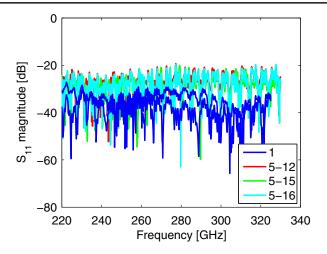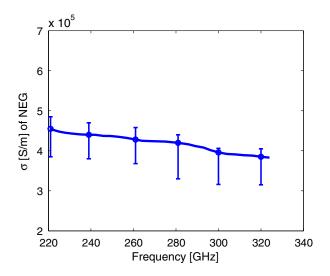

FIG. 8. NEG effective conductivity between 220–330 GHz as extracted from the intersection of measurements and CST simulations assuming a uniform coating of 3 μm.

extracted from CST simulations considering a uniform coating of 3 μm as described in Sec. II. The results between 220–330 GHz are shown in Fig. 8.

For lower frequencies around 220 GHz, a 15% difference can be noticed between the DC conductivity value of 0.57×10^6 S/m and the extracted value. Measurements along the waveguide with an optical profilometer revealed an average roughness Rq of 0.2 μm. Assuming a conductivity of $\sigma = 0.57 \times 10^6$ S/m, the skin depth would vary between 1.4 μm and 1.15 μm across the frequency range. The observed difference at lower frequencies lies within the uncertainty of the experimental method and the error of the DC conductivity measurement itself. However, at higher frequencies up to 330 GHz the difference increases to around 32%, indicating a clear frequency dependence for the conductivity. From estimates found using CST, surface roughness effects are expected to contribute to a reduction in conductivity in the order of 5% for a roughness of Rq = 0.2 μm.

V. MEASUREMENTS AT 500–750 GHz

Measurements were also conducted for frequencies between 500–750 GHz with two WR1.5 waveguides labeled as 4–26 and 4–27. The dimensions of the waveguides are 0.381 mm in width and 0.191 mm in height. The results are shown in Fig. 9.

The transmission of sub-THz signals can be severely affected by water in the atmosphere. Many strong absorption lines are observed in the THz region [14]. One of them was recorded during our measurements at 557 GHz. It appears as a sharp decrease in S_{21} in Fig. 9. In the same figure S_{21} measurements are compared to CST simulations (magenta) for a smooth 3 μm NEG-coated waveguide with a DC conductivity of 0.57×10^6 S/m.

FIG. 10. Measurements of the reflection parameters S_{11}. The return loss remains below −15 dB between 500–700 GHz and only at frequencies above 700 GHz S_{11} is around −15 dB.

The reflection parameters S_{11} were also measured with the waveguides in forward and reverse direction and the results are shown in Fig. 10. The return loss remains below −15 dB for frequencies between 500–700 GHz, and only for frequencies above 700 GHz does the measured value of S_{11} exceed −15 dB. At this point a small effect might be observed on the transmission signal S_{21} marking the delicacy of such high frequency measurements.

The effective conductivity extracted from the intersection between the measured data and values found from CST simulations assuming a uniform coating of 3 μm is shown in Fig. 11.

A 38% difference from the DC conductivity is observed at 500 GHz, while the difference increases to 62% at 750 GHz. Roughness of Rq = 0.3 μm was measured along
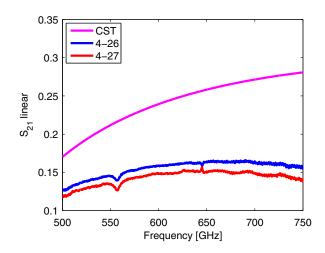

FIG. 9. S_{21} CST simulation (magenta) for a DC conductivity value of 0.57×10^6 S/m compared with transmission coefficient measurements along two WR1.5 waveguides. The waveguides are labeled as 4–26 (blue) and 4–27 (red).
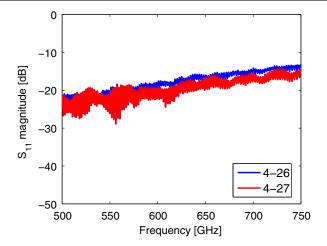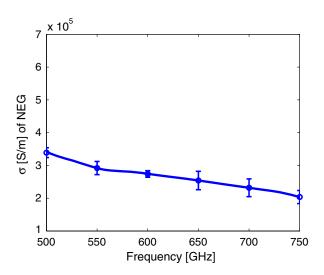

FIG. 11. NEG effective conductivity between 500–750 GHz as extracted from the intersection of measured data and CST simulation assuming a uniform coating of 3 μm.

the WR1.5 waveguides with the profilometer. The reduction in conductivity predicted by CST simulations is 23% for a roughness of Rq = 0.3 μm. Similar to the 220–330 GHz regime shown in Fig. 8, the extracted results indicate a significant decrease in conductivity with increasing frequency, whilst roughness effects do not seem to be adequate to explain such a reduction.

The hypothesis made previously was that the NEG coating thickness is constant along the waveguide and equal to the targeted thickness of 3 μm. In order to investigate whether the observed reduction of conductivity was due to an intrinsic property of the NEG coating or if it was due to an incorrect assumption for the coating thickness in the CST simulations, further studies were carried out.

VI. EFFECT OF THE NONUNIFORM PROFILE

A significant reduction of the conductivity with increasing frequency of around 32% at 330 GHz and 62% at 750 GHz was detected as shown in Figs. 8 and 11. Such a big reduction cannot be explained by roughness alone, while relaxation effects are not typically expected below 10^{14} Hz for metals [15]. The Drude model [16] is used to express the frequency dependent conductivity σ_c when the conventional constant conductivity model is no longer valid. It is given by

$$\sigma_c = \frac{\sigma}{1 + j2\pi f \tau}, \tag{3}$$

where σ is the DC conductivity and τ the mean free time. For most conductors the mean free time τ^{-1} is in the range of 10^{13} to 10^{14} Hz [17], while our measurements extend up to 7.5×10^{11} Hz.

Further studies were necessary to acquire a better understanding of the observed conductivity behavior with frequency which conventional theory could not explain.

A. Coating profile measurements

A systematic feature that was not previously considered in the CST simulations is the nonuniformity of the coating profile. So far it was assumed to be uniform, i.e., with a constant thickness. However, scanning electron microscope (SEM) analysis revealed very nonuniform profiles in all WR3.4 and WR1.5 waveguides.

The analysis on a WR3.4 waveguide width showed a variation of between 5 μm in the corners to 10 μm in the center. On the side walls, which is the least preferential direction for the chosen coating method, it varied between 1 μm and 3 μm. The targeted thickness was 3 μm, but as the SEM analysis revealed, the actual profile varied significantly.
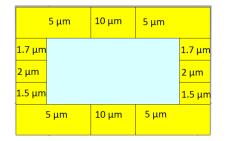

FIG. 12. Front view of a WR3.4 waveguide in CST separated into various blocks with different NEG thickness. Along the width of the groove, 5 μm and 10 μm are used. On the side walls 1.5 μm, 1.7 μm, and 2 μm are used according to the SEM results.

B. CST simulation of the variable coating thickness

In order to investigate the effect of the nonuniform profile, a different approach for the CST simulations was followed. The idea is to divide the waveguide into smaller blocks, and to simulate a coating of different thickness in each block according to the profile measurements. Along the width, 5 μm and 10 μm are considered. Along the height of the waveguide, 1.5 μm, 1.7 μm, and 2 μm are used, as determined from the SEM analysis. The front view of the new waveguide setup can be seen in Fig. 12.

The result of the intersection of CST simulations assuming a nonuniform profile with the measured data is shown in Fig. 13. The conductivity now varies by around 3% in the measured frequency range. Hence, a negligible frequency dependency is observed compared to the variation found in Fig. 8 when the hypothesis of a uniform coating was used in CST.

From the results shown in Fig. 13 it is clear that the nonuniformity of the NEG coating thickness plays a crucial role in the extracted conductivity results. The CST
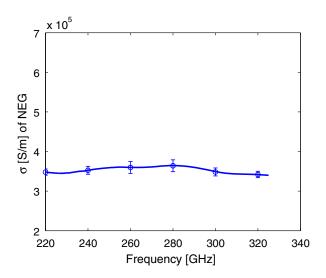

FIG. 13. NEG effective conductivity between 220–330 GHz as extracted from the intersection of measurements and CST simulation for a nonuniform profile.
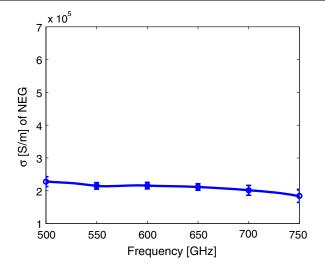
FIG. 14.   NEG effective conductivity between 500–750 GHz as extracted from the intersection of measurements and CST simulation with a nonuniform profile according to the SEM results.
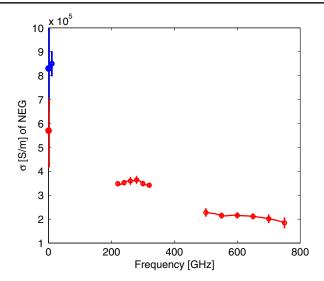

FIG. 15.   Extracted NEG conductivity between 10–11 GHz, 220–330 GHz, and 500–750 GHz. For the measurements in blue, the X-band coating setup was used to apply the NEG film while for the measurements in red the coating setup for small dimension objects was used. The DC measurements are also included in the plot and shown at 0 GHz. A difference is observed even for the DC conductivity (blue and red at 0 GHz) depending on the coating setup used. The NEG conductivity seems to reduce as frequency increases by a factor 2–3 times compared to the DC value.

simulation that accounted for the real profile of the coating shown in Fig. 12 proved that the conductivity drop versus frequency obtained in Fig. 8 disappears once the profile is set to nonuniform.

A similar procedure was followed for the WR1.5 waveguide using SEM measurements of the actual coating thickness, with the extracted conductivity shown in Fig. 14. In this case, the SEM analysis for the WR1.5 waveguide showed a variation across the width of between 4 μm in the corners and 7 μm in the center, and between 0.5 μm and 1.5 μm on the side walls.

The extracted conductivity now reduces by around 13% along the frequency range of 500–750 GHz as shown in Figure 14 which is significantly less than in Figure 11. Nevertheless, it is still noticeable but within the expected reduction due to the contribution of surface roughness.

VII. CONCLUSIONS

An experimental method was used to characterize the effective conductivity of NEG at frequencies of a few hundreds of GHz for the first time. As a first step, the principle of the method was demonstrated for stainless steel waveguides in X-band and for a bare gold waveguide in the frequency range of 220–330 GHz. The method gave results that are in very good agreement with the expected DC conductivity for the two metals, whilst at the same time indicated that roughness effects cannot be neglected at very high frequencies.

The same method was then applied in order to characterize the NEG conductivity. All results obtained with this method are summarized in Fig. 15.

At lower frequencies between 10 GHz and 11 GHz the extracted conductivity agrees well with the DC value. It was noticed that the way the coating is applied plays a role in the DC conductivity of the NEG coating as it affects the elemental composition of the alloy. The difference of the DC conductivity depending on the coating method can be seen in Fig. 15 at 0 GHz. In this, the red and blue markers indicate different methods used to apply the NEG coating, depending upon the dimensions of the object to be coated.

For the higher frequency measurements all waveguides were coated with NEG using the second method and are shown in red. The extracted NEG conductivity can be 1.5 times lower than the DC value due to the effect of surface roughness and nonuniformity of the coating profile. The reduction becomes more significant in the frequency range of 500–750 GHz, where the factor is around 2.5. Roughness effects can explain around 5% and 20% reduction in conductivity between 220–330 and 500–750 GHz, respectively.

Including a more realistic coating profile in CST simulations was proved to be extremely important for the correct determination of conductivity behavior versus frequency.

The nonuniformity of the coating is expected to be less severe in accelerator vacuum chambers compared to the thickness variation reported in these measurements using rectangular waveguides. The latter structure is particularly hard to coat in a uniform way due to its geometry. A different coating system with the possibility of rotating the sample across the source could provide a solution to this problem.

An important conclusion from this study is that the effective conductivity at high frequencies can be lower than the DC values, and that surface roughness effects cannot be neglected. Therefore, a more accurate conductivity model should be considered for beam dynamics simulations when the beam frequency spectrum extends to high frequencies.

ACKNOWLEDGMENTS

[1] C. Benvenuti, P. Chiggiato, P. C. Pinto, A. E. Santana, T. Hedley, A. Mongelluzzo, V. Ruzinov, and I. Wevers, Vacuum properties of TiZrV non-evaporable getter films, Vacuum **60,** 57 (2001).

[2] C. Benvenuti, P. Chiggiato, P. C. Pinto, A. Prodromides, and V. Ruzinov, Influence of the substrate coating temperature on the vacuum properties of Ti–Zr–V non-evaporable getter films, Vacuum **71,** 307 (2003).

[3] M. S. Pambianchi, L. Chen, and S. M. Anlage, Complex conductivity of proximity-superconducting Nb/Cu bilayers, Phys. Rev. B **54,** 3508 (1996).

[4] A. Gustafsson, S. Calatroni, W. Vollenberg, and R. Seviour, in *Proceedings of the International Particle Accelerator Conference, Kyoto, Japan* (ICR, Kyoto, 2010), p. WEPEC047.

[5] C. Benvenuti, P. Chiggiato, F. Cicoira, and V. Ruzinov, Decreasing surface outgassing by thin film getter coatings Vacuum, **50,** 57 (1998).

[6] C. Benvenuti, in *Proceedings of the 6th European Particle Accelerator Conference, Stockholm, 1998* (IOP, London, 1998), p. 299.

[7] CST Microwave Studio- Getting Started (2003).

[8] K. Kurokawa, Power Waves and the Scattering Matrix, IEEE Trans. Microwave Theory Tech. **13,** 194 (1965).

[9] D. K. Cheng, in *Field and Wave Electromagnetics*, 2nd ed. (Pearson Education, Boston, 1989).

[10] E. Koukovini-Platia, G. Rumolo, and C. Zannini, in *Proceedings of International Particle Accelerator Conference* (JACoW, Geneva, 2014), p. WEPME050.

[11] E. Koukovini-Platia, École Polytechnique Fédérale de Lausanne, Ph.D. thesis; Report No. CERN-THESIS-2015-152 (2015), p. 61.

[12] N. N. Rao, in *Elements of Engineering Electromagnetics*, 4th ed. (Prentice Hall, Englewood Cliffs, 1994).

[13] E. Koukovini-Platia, École Polytechnique Fédérale de Lausanne, Ph.D. thesis; Report No. CERN-THESIS-2015-152 (2015), p. 65–67.

[14] S. Paine, The am atmospheric model, SMA technical memo 152, version 9, Smithsonian Astrophysical Observatory (2016).

[15] S. Calatroni, in *Low Emittance Rings 2014 Workshop, Frascati* (2014).

[16] H. Booker, *Energy in Electromagnetism*, 1st ed. (Peter Peregrinus, London, 1982).

[17] C. Kittel, *Introduction to Solid State Physics* (John Wiley & Sons, New York, 1986).